Feifei Zhang, Qi Gao, Junxia Zhao, Man Ge and Yinjuan Bai*

Design and synthesis of a novel rhodamine-based chemosensor and recognition study to Fe^{3+}

DOI 10.1515/hc-2015-0139
Received July 7, 2015; accepted September 19, 2015; previously published online January 12, 2016

Abstract: A fluorescent and colorimetric chemosensor **Rh1** for Fe^{3+} was synthesized by condensation reaction of rhodamine B hydrochloride and 2-aminothiazole, and its structure was confirmed by NMR, IR, HRMS and crystal data. Upon coordination with Fe^{3+} in CH_3CN-H_2O (1:1, v/v) solution, the spirolactam of **Rh1** is opened, which results in a dramatic enhancement of fluorescence intensity as well as the color change of the solution. Most importantly, other metal ions show no obvious interference with the detection of Fe^{3+}. Under the optimum conditions described, the fluorescence intensity is linearly proportional to the concentration of Fe^{3+} in the range of 2 μM ~ 7 μM. The Job's plot indicates a 1:1 binding stoichiometry between **Rh1** and Fe^{3+}. The association constant (Ka) is 2.26×10^4 M^{-1}.

Keywords: Fe^{3+}; fluorescent chemosensor; fluorescence intensity; spirolactam.

Introduction

Iron is one of the most essential trace elements in biological systems being involved in enzymatic reactions, muscle contraction, nerve conduction, electron transfer and transport of oxygen through heme [1–3]. Iron can also promote the process of cellular metabolism and the synthesis of DNA and RNA [4–6]. There are many evidences indicating that either deficiency or overload of Fe^{3+} can induce biological disorders in living body. For example, lack of iron in the blood can cause serious anemia. On the other hand, overload of iron ion has also been associated with certain cancers and dysfunction of liver, heart and nervous system [7, 8]. Thus far, many methods such as atomic absorption spectroscopy (AAS) [9, 10], inductively coupled plasma-atomic emission spectroscopy (ICP-AES) [11, 12], voltammetry [13] and inductively coupled plasma-mass spectroscopy (ICP-MS) [14] have been used to determinate Fe^{3+}. Although these methods are both quantitative and highly-sensitive, they are not suitable for using in real-time and on-site detection of Fe^{3+}. Fluorescent methods have gained much attention of researchers due to their good selectivity and recognition, rapid response and application in the environment of organisms [15–17]. Many excellent fluorescent chemosensors for Fe^{3+} have been reported in the past few years [18–23]. Although most of them have superior detection performance, some of them suffer drawbacks including low tolerance of Cu^{2+} and Cr^{3+}, low sensitivity and inconspicuous change in color, which restrict the application of these sensors in biological systems. Additionally, many Fe^{3+}-selective fluorescent probes are usually based on fluorescence quenching mechanism [24–26]. These probes are easily influenced by background and other factors. Therefore, it is important to design 'off-on' fluorescent chemosensors for Fe^{3+} with color and fluorescence changes in aqueous solution.

Rhodamine skeleton, which has excellent photophysical properties like long absorption and emission wavelength, high fluorescence quantum yield, high molar extinction coefficient and good photostability, has attracted great interest. More importantly, rhodamine derivatives exist in a spirolactam form with weak fluorescence under the neutral or alkaline conditions but can undergo ring opening in the presence of certain metal ions, and the opened form is strongly fluorescent. Therefore, rhodamine framework has become an ideal model to construct 'off-on' fluorescent chemosensors. Furthermore, electron donors (such as N, S) are usually introduced to the probes to improve the chelator's affinity toward metal ions [27]. Thiazoles and their derivatives have been considered as an important class of S and N-containing heterocycles [28]. They can form bi- or multinuclear complexes with transition metal ions [29]. Herein, on the basis of the photo-induced electron transfer (PET) mechanism, we designed a new fluorescent chemosensor **Rh1** by using rhodamine B as a fluorophore and an aminothiazole moiety as a Fe^{3+} chelator (Scheme 1). The structure of

***Corresponding author: Yinjuan Bai,** Key Laboratory of Synthetic and Natural Functional Molecule Chemistry of Ministry of Education, College of Chemistry and Materials Science, Northwest University, Xi'an, Shaanxi 710127, PR China, e-mail: baiyinjuan@nwu.edu.cn
Feifei Zhang, Qi Gao, Junxia Zhao and Man Ge: Key Laboratory of Synthetic and Natural Functional Molecule Chemistry of Ministry of Education, College of Chemistry and Materials Science, Northwest University, Xi'an, Shaanxi 710127, PR China

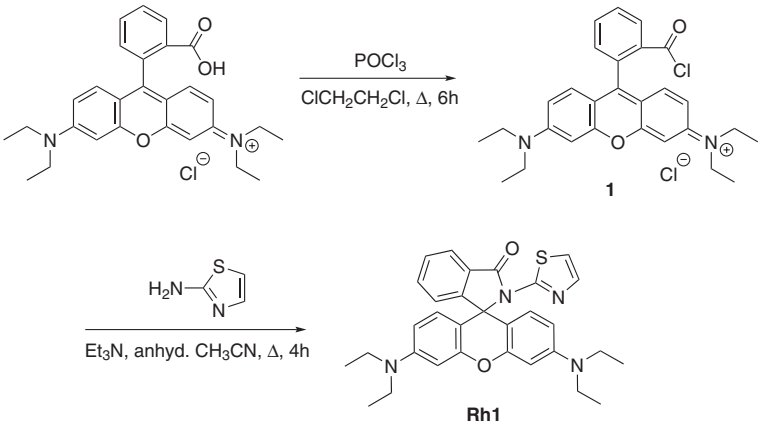

Scheme 1 Synthesis of **Rh1**.

Rh1 was confirmed by X-ray crystallographic analysis in addition to NMR data. The sensitive chemosensor **Rh1** can selectively detect Fe^{3+} in CH_3CN-H_2O (1:1, v/v) solution and can be used in the presence of Cr^{3+} and Cu^{2+} .

Results and discussion

The given structure of **Rh1** was confirmed by X-ray crystallographic analysis (Figure 1). White single crystal of **Rh1** was obtained by slow concentration at room temperature of the dichloromethane–acetonitrile solution. Single-crystal X-ray diffraction structural analysis indicates that **Rh1** crystallizes in orthorhombic system and the space group is Pbca without a symmetric center. Two spiro planes of the rhodamine frame-work are coordinated in mutually vertical positions. Additional crystallographic data and structural refinements for **Rh1** are shown in the Supporting Information.

In order to examine the selectivity of **Rh1**, spectroscopic studies in the presence of various metal cations were conducted in CH_3CN-H_2O (1:1, v/v) solution. As shown in Figure 2, in the absence of Fe^{3+} ion, the sensor **Rh1** (20 μM) shows a very weak fluorescence which can be ascribed to the probe mainly existing in the form of spirolactam. Upon binding with Fe^{3+}, **Rh1** exhibits an intense fluorescent emission at 580 nm. Moreover, the colorless solution develops a pink color (Figure 3). Under similar conditions, the addition of other metal ions including K^+, Na^+, Li^+, Ag^+, Ca^{2+}, Ba^{2+}, Mg^{2+}, Zn^{2+}, Cd^{2+}, Mn^{2+}, Co^{2+}, Ni^{2+}, Cu^{2+}, Hg^{2+}, Fe^{2+}, Al^{3+} and Cr^{3+} does not induce any visible fluorescence or color changes in the absence of ferric ion. This specific feature demonstrates that probe **Rh1** shows excellent recognition toward Fe^{3+} ion in the presence of

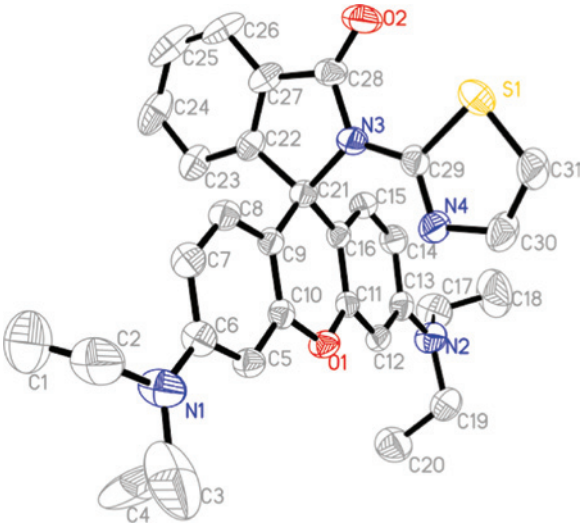

Figure 1 Crystal structure of sensor **Rh1**.

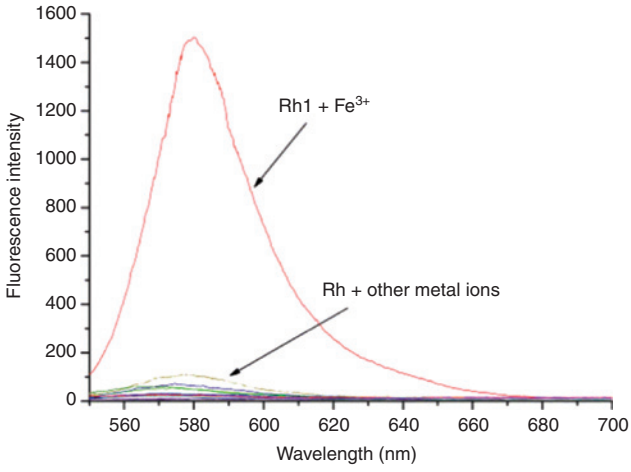

Figure 2 Fluorescence response of probe **Rh1** (20 μmol/L) to different metal ions (20 μmol/L).

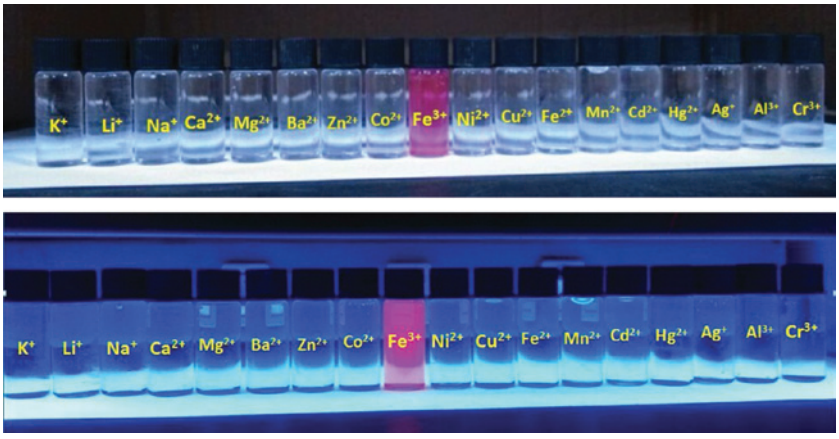

Figure 3 The colorimetric (top) and fluorometric (bottom) changes of **Rh1** (20 μM) upon addition of Fe^{3+} and other cations in CH_3CN-H_2O (1:1, v/v) solution (20 μM for Fe^{3+} and other cations). The two photos were obtained in sunlight (top) and upon irradiation with a 365-nm UV lamp (bottom).

other cations and can be used for naked-eye detection. In addition, the interference experiments of **Rh1** were also conducted (Figure S4 in the Supporting Information). In these experiments, the fluorescence changes of **Rh1** in CH_3CN-H_2O (1:1, v/v) solution were measured by the treatment of 20 μM Fe^{3+} ion in the presence of 100 equiv. of other cations. In the presence of other metal ions, the fluorescence intensity of the **Rh1**- Fe^{3+} complex had no significant variation regardless of whether there were other metal ions.

To further investigate the influence of Fe^{3+} on **Rh1**, a fluorescence titration experiment at different Fe^{3+} concentrations was carried out. As shown in Figure 4, free **Rh1** exhibits a very slight fluorescence, which is due to the efficient photoinduced electron transfer (PET) process from the electron-rich receptor aminothiazole moiety to the excited rhodamine fluorophore. Upon addition of Fe^{3+}, the PET mechanism is quenched and, as a result, the fluorescent emission peak at 580 nm increases in intensity. The increase of fluorescent emission becomes saturated in the presence of 1.5 equiv. of Fe^{3+}. Moreover, a good linear relationship between the fluorescence emission intensity of **Rh1** and the concentration of Fe^{3+} in the range of 2 μM ~ 7 μM can be noted (Figure S5). The regression equation is

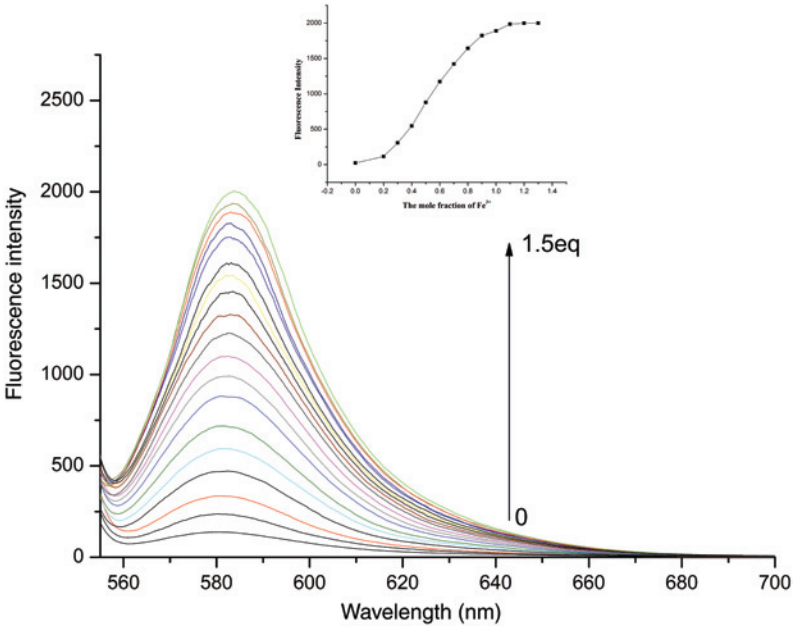

Figure 4 Fluorescence emission spectra of **Rh1** (20 μM) in the presence of increasing concentrations of Fe^{3+}. The inset shows emission intensity at λ_{em} = 580 nm as a function of Fe^{3+} concentration (λ_{ex} = 545 nm).

$Y = 2264.8X - 92.075$, $R^2 = 0.9978$. Based on the expression $3 \times \delta_{blank}/k$ (where δ_{blank} is the standard deviation of the blank solution and k is the slope of the calibration curve), the limit of detection was calculated to be 2.43×10^{-8} M. A Job's plot for the fluorescent was applied at room temperature to determine the stoichiometry of **Rh1** and Fe^{3+}. Keeping the sum of the initial concentration of Fe^{3+} and **Rh1** at 20 μM, the molar ratio of Fe^{3+} was varied from 0 to 1. As shown in Figure 5, the maximum emission intensity is obtained at a molar ratio of 0.5. This indicated that **Rh1** chelates Fe^{3+} with a 1:1 stoichiometry. The association constant (Ka) for **Rh1** and Fe^{3+} was also measured using the Benesi–Hildebrand method (Figure 6). The estimated Ka value is 2.26×10^4 M^{-1}.

Besides, it was interesting to investigate the reversible binding nature of the sensor (Figure 7). Upon addition of

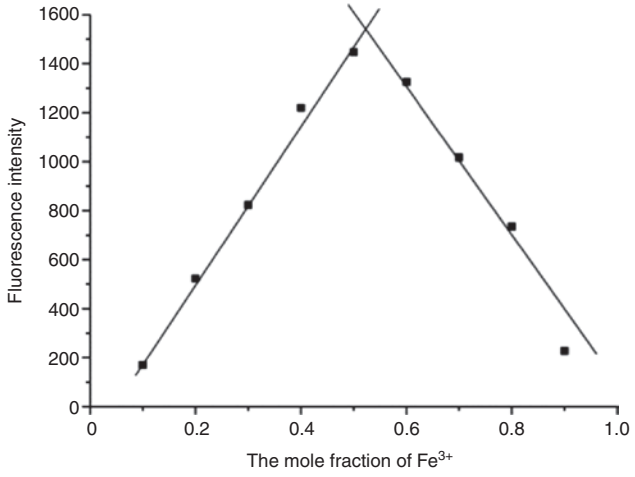

Figure 5 Job's plot of probe **Rh1** and Fe^{3+}.

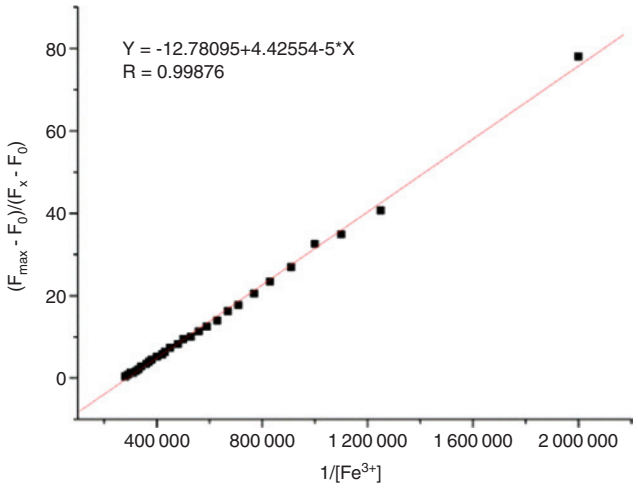

Figure 6 Benesi-Hildebrand plot of **Rh1** assuming 1:1 binding stoichiometry with Fe^{3+} (λ_{ex} = 545 nm, λ_{em} = 580 nm).

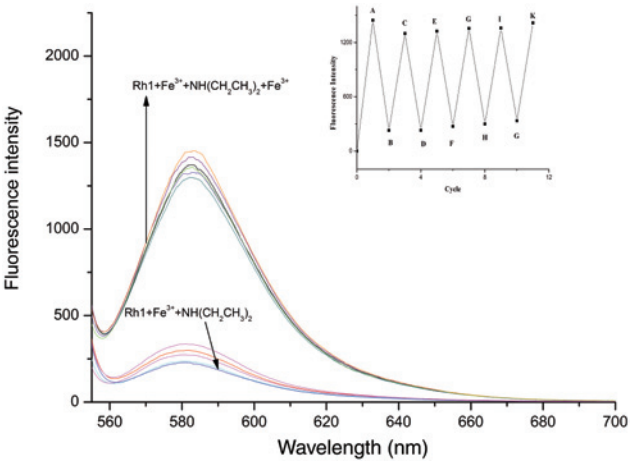

Figure 7 Fluorescence intensity of the system **Rh1** + Fe^{3+} as a function of $NH(CH_2CH_3)_2$ concentration in CH_3CN-H_2O (1:1, v/v) solution. Inset shows reversible complexation/decomplexation cycles carried out with **Rh1** and Fe^{3+} (λ_{ex} = 545 nm, λ_{em} = 580 nm).

ethylenediamine (20 μM) to the solution of **Rh1** (20 μM) and Fe^{3+} (20 μM), the fluorescence intensity at 580 nm decreased (A→B) due to the competitive binding of Fe^{3+} from **Rh1** by ethylenediamine and formation of the spirolactam. The strong fluorescence was observed again (B→C) upon further addition of 20 equiv. Fe^{3+}. As can be seen, this sequence was followed five times without any change in intensity. This results shows that complexation of **Rh1** with Fe^{3+} is chemically reversible.

To understand the structural change of **Rh1** upon the complexation with ferric ion, molecular modeling was performed using DFT calculations at B3LYP/6-31G level with the Gaussian 09 program [30, 31] (Figure 8). Combined with Figure 8 and PET mechanism [32], it can concluded that in the absence of Fe^{3+}, the HOMO of the electron-rich receptor aminothiazole moiety has a higher energy than the half-filled HOMO of the excited rhodamine fluorophore. This energy difference drives a rapid electron transfer from the aminothiazole moiety to the excited-state rhodamine fluorophore, which inhibits the intrinsic fluorescence of the rhodamine and, as a result, the probe exhibits a weak fluorescence. Upon addition of Fe^{3+}, this cation interacts with the lone-pair electrons on the nitrogen atoms of the aminothiazole moiety and the rhodamine fluorophore undergoes opening of the spiro-ring. The energy level of the aminothiazole moiety is lower than that of the HOMO of the excited rhodamine fluorophore, and the electron delocalization is not energetically favored. The exited electron of rhodamine fluorophore is returned to the stationary state and the fluorescence is 'switched on'.

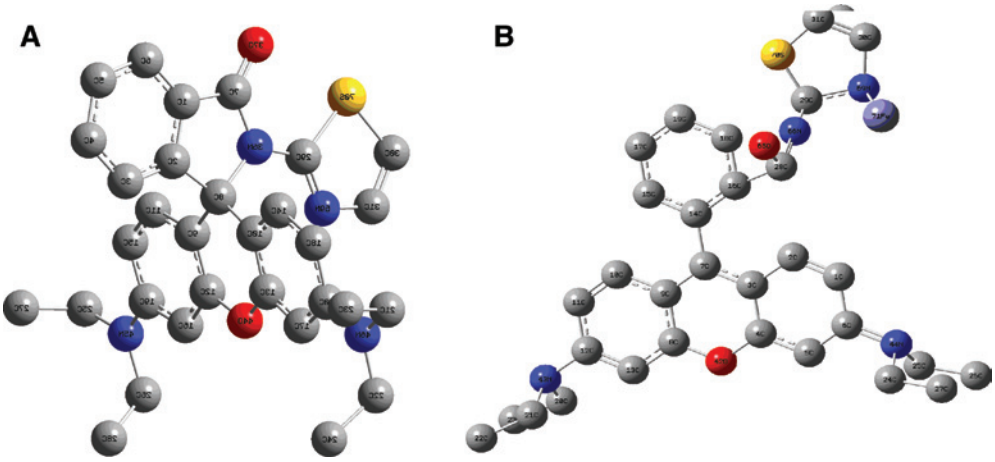

Figure 8 The energy-minimized structure of free **Rh1** molecule (A) and the **Rh1**-Fe^{3+} complex (B).

Conclusion

An 'off-on' fluorescent chemosensor based on rhodamine has been synthesized. It exhibits an excellent selectivity and a high sensitivity to the detection of Fe^{3+} in CH_3CN-H_2O (1:1, v/v) solution. The sensor is also suitable for visual detection of ferric ion. The fluorescence intensity and the concentration of Fe^{3+} have a linear relationship in the range of 2 μM ~ 7 μM. The detection limit is 2.43×10^{-8} M and the association constant (Ka) for **Rh1** and Fe^{3+} is 2.26×10^4 M^{-1}.

Experimental

The fluorescent spectra were recorded on a HITACHI F-4500 fluorescence spectrophotometer. X-ray crystal data were collected on Bruker Smart APEX II CCD diffractometer. All solvents and reagents (analytical grade) were purchased from commercial suppliers and used without further purification. Double distilled water was used. The solutions of metal ions were prepared from corresponding nitrate and chloride salts. Stock solutions of **Rh1** (1 mM) were prepared in acetonitrile. Stock solutions of the metal ions (10 mM) were prepared in double distilled water with the metal salts KCl, NaCl, LiCl, $MgCl_2$, $BaCl_2$, AgCl, $CaCl_2$, $ZnCl_2$, $CdCl_2$, $Cu(NO)_3$, $MnCl_2$, $CoCl_2$, $NiCl_2$, $FeCl_2$, $Al(NO)_3$, $FeCl_3$, $HgCl_2$ and $CrCl_3$.

Synthesis of Rh1

To a stirred solution of rhodamine B hydrochloride (1.92 g, 4 mmol) in 1,2-dichloroethane (20 mL), 3 mL phosphorus oxychloride was added. The solution was heated under reflux for 6 h and then concentrated. The resultant crude acid chloride was dissolved in 10 mL acetonitrile and the solution was treated dropwise with a solution of 2-aminothiazole (4 mmol) and triethylamine (1 mL) in acetonitrile (10 mL). The mixture was heated under reflux for 5 h, cooled to room temperature and poured into 50 mL cold water. After extraction with dichloromethane, the extract was washed with saturated aqueous NaCl solution, dried over anhydrous $MgSO_4$ and concentrated. The residue was purified by silica gel chromatography eluting with ethyl acetate/petroleum ether (1:5, v/v) to give 0.71 g white powder: yield 35%; mp 238–240°C; ^{1}H NMR (400 MHz, CD_3Cl): 1.14 (t, 12H, J = 7.2 Hz), 3.29 (q, 8H, J = 7.2 Hz), 6.15 (dd, 2H, J_1 = 8.8 Hz, J_2 = 2.4 Hz), 6.38 (d, 2H, J = 8.8 Hz), 6.42 (d, 2H, J = 2.8 Hz), 6.80 (d, 1H, J = 3.6 Hz), 7.18 (d, 1H, J = 7.2 Hz), 7.25 (d, 1H, J = 3.8 Hz), 7.48–7.58 (m, 2H), 8.03 (d, 1H, J = 6.8 Hz); ^{13}C NMR (100 MHz, CD_3Cl): 11.6, 43.2, 66.5, 96.4, 105.3, 106.2, 111.4, 122.3, 123.6, 126.9, 127.5, 127.8, 133.1, 137.5, 147.7, 152.7, 152.8, 154.1, 165.5; IR (KBr)**:** 3440, 3106, 3098, 2971, 1933, 1702, 1612, 1542, 1513, 1461, 1330, 1224, 1186, 1120, 831, 777, 696 cm^{-1}. ESI-HR-MS. Calcd for ($M+H^+$): m/z 525.2319. Found: m/z 525.2312.

X-ray crystal structure determination of compound Rh1

The crystal data has been collected at 296 K by using Mo Ka radiation (λ = 0.71073 Å) in the θ range of 2.10°–25.10°, a scan mode and collection for Lorentz and polarization effect (SADABS). The structure was solved using the direct method and refined by full-matrix least-squares fitting on F2 by SHELX-97. Crystallographic data have been deposited to the Cambridge Crystallography Data Center with deposition number of 1403579 for compound **Rh1**.

Supporting information

Online-only supplementary data include fluorescence spectra for **Rh1**.

Acknowledgments: We gratefully acknowledge financial support from the National Natural Science Foundation of China (No. 21042002).

References

[1] Papanikolaou, G.; Pantopoulos, K. Iron metabolism and toxicity Toxicol. *Appl. Pharmacol.* **2005**, *202*, 199–211.

[2] D'Autreáux, B.; Tucker, N. P.; Dixon, R.; Spiro, S.A. Non-heam iron centre in the transcription factor NorR senses nitric oxide. *Nature* **2005**, *437*, 769–772.

[3] Wessling-Resnick, M. Biochemistry of iron uptake. *Crit. Rev. Biochem. Mol. Biol*. **1999**, *34*, 285–314.

[4] Weizman, H.; Ardon, O.; Mester, B.; Libman, J.; Dwir, O.; Hadar, Y.; Chen, Y.; Shanzer, A. Fluorescently-labeled ferrichrome analogs as probes for receptor-mediated, microbial iron uptake. *J. Am. Chem. Soc*. **1996**, *118*, 12368–12375.

[5] Sumner, J. P.; Kopelman, R. Alexa Fluor 488 as an iron sensing molecule and itsapplication in PEBBLE nanosensors. *Analyst* **2005**, *130*, 528–533.

[6] Dornelles, A. S.; Garcia, V. A.; de Lima, M. N.; Vedana, G.; Alcalde, L. A.; Bogo, M. R.; Schroeder, N. mRNA expression of proteins involved in iron homeostasis in brainregions is altered by age and by iron overloading in the neonatal period. *Neurochem. Res*. **2010**, *35*, 564–571.

[7] Kozlowski, H. A.; Janicka-Klos, J.; Brasun, E.; Gaggelli, D.; Valensin, G. Valensin copper, iron, and zinc ions homeostasis and their role in neurodegenerative disorders (metal uptake, transport, distribution and regulation). *Coord. Chem. Rev*. **2009**, *253*, 2665–2685.

[8] Crichton, R. R.; Dexter, D. T.; Ward, R. J. Metal based neurodegenerative diseases–from molecular mechanisms to therapeutic strategies. *Coord. Chem. Rev*. **2008**, *252*, 1189–1199.

[9] Kobayashi, H.; Ogawa, M.; Alford, R.; Choyke, P. L.; Urano, Y. New strategies for fluorescent probe design in medical diagnostic imaging. *Chem. Rev*. **2010**, *110*, 2620–2640.

[10] Singh, A.; Sinha, S.; Kaur, R.; Kaur, N.; Singh, N. Rhodamine based organic nanoparticles for sensing of Fe^{3+} with high selectivity in aqueous medium: application to iron supplement analysis. *Sens. Actuators, B.* **2014**, *204*, 617–621.

[11] Pomazal, K.; Prohaska, C.; Steffan, I.; Reich, G.; Huber, J. F. K. Determination of Cu, Fe, Mn, and Zn in blood fractions by SEC-HPLC-ICP-AES coupling. *Anal.* **1999**, *124*, 657–663.

[12] Wang, J.; Zhang, D.; Liu, Y.; Ding, P.; Wang, C.; Yea, Y.; Zhao, Y. F. A N-stablization rhodamine-based fluorescent chemosensor for Fe^{3+} in aqueous solution and its application in bioimaging. *Sens. Actuators, B*. **2014**, *191*, 344–350.

[13] Lunvongsa, S.; Oshima, M.; Motomizu, S. Determination of total and dissolved amount of iron in water samples using catalytic spectrophotometric flow injection analysis. *Talanta* **2006**, *68*, 969–973.

[14] Dadfarnia, S.; Haji Shabani, A. M.; Gohari, M. Trace enrichment and determination of silver by immobilized DDTC microcolumn and flow injection atomic absorption spectrometry. *Talanta* **2004**, *64*, 682–687.

[15] Bhalla, V.; Sharma, N.; Kumar, N.; Kumar, M. Rhodamine based fluorescence turn-on chemosensor for nanomolar detection of Fe^{3+} ions. *Sens. Actuators, B*. **2013**, *178*, 228–232.

[16] van den Berg, C. M. G. Chemical speciation of iron in seawater by cathodic stripping voltammetry with dihydroxynaphthalene. *Anal. Chem.* **2006**, *78*, 156–163.

[17] Wei, Y.; Qin, G.; Wang, W.; Bian, W.; Shuang, S.; Dong, C. Development of fluorescent Fe(III) sensor. *J. Lumin.* **2011**, *131*, 1672–1676.

[18] Du, J. J.; Fan, J. L.; Peng, X. J.; Sun, P. P.; Wang, J. Y.; Li, H. L.; Sun, S. G. A new fluorescent chemodosimeter for Hg^{2+}: selectivity, sensitivity, and resistance to Cys and GSH. *Org. Lett.* **2010**, *12*, 476–479.

[19] Lee, M. H.; Giap, T. V.; Kim, S. H.; Lee, Y. H.; Kang, C.; Kim, J. S. A novel strategy to selectively detect Fe(III) in aqueous media driven by hydrolysis of a rhodamine 6G Schiff base. *Chem. Commun.* **2010**, *46*, 1407–1409.

[20] Xi, P.; Dou, J.; Huang, L.; Xu, M.; Chen, F. J.; Wu, Y.; Bai, D.; Li, W.; Zeng, Z. Z. A selective turn-on fluorescent sensor for Cu(II) and its application in imaging in living cells. *Sens. Actuators B.* **2010**, *148*, 337–341.

[21] Bordini, J.; Calandreli, I.; Silva, G. O.; Ferreira, K. Q.; Leitão-Mazzi; D. P. S.; Espreafico, E. M.; Tfoun, E. A rhodamine-B-based turn-on fluorescent sensor for biological iron(III). *Inorg. Chem. Commun.* **2013**, *35*, 255–259.

[22] Fegade, U.; Singh, A.; Chaitanya, G. K.; Singh, N.; Attarde, S.; Kuwar, A. Highly selective and sensitive receptor for Fe^{3+} probing. *Spectr. Acta A.* **2014**, *121*, 569–574.

[23] Wang, S. X.; Meng, X. M.; Zhu, M. Z. A naked-eye rhodamine-based fluorescent probe for Fe(III) and its application in living cells. *Tetrahedron Lett.* **2011**, *52*, 2840–2843.

[24] Bricks, J. L.; Kovalchuk, A.; Trieflinger, C.; Nofz, M.; Bueschel, M.; Tolmachev, A. I.; Daub, J.; Rurack, K. On the development of sensor molecules that display FeIII-amplified fluorescence. *J. Am. Chem. Soc.* **2005**, *127*, 13522–13529.

[25] Xiang, Y.; Tong, A. J. A new rhodamine-based chemosensor exhibiting selective FeIII-amplified fluorescence. *Org. Lett.* **2006**, *8*, 1549–1552.

[26] Fan, L. J.; Zhang, Y.; Jones, W. E. Design and synthesis of fluorescence "Turn-on" chemosensors based on photoinduced electron transfer in conjugated polymers. *Macromolecules* **2005**, *38*, 2844–2849.

[27] Li, J.; Zhang, C. F.; Ming, Z. Z.; Hao, G. F.; Yang, W. C.; Yang, G. F. Coumarin-based novel fluorescent zinc ion probe in aqueous solution. *Tetrahedron* **2013,** *69*, 4743–4748.

[28] Livingstone, S. E. Other Sulfur-Containing Ligands. In *Ligands, Comprehensive Coordination Chemistry*. Wilkinson, G., Gillard, R. D., McCleverty, J. A. Eds. Pergamon Press: Oxford, 1987; Vol. 2.

[29] Kuang, S. M.; Zhang, Z. Z.; Xue, F.; Mak, T. C. W. Directional Fe–C/O···S intermolecular interaction leading to chain-like crystal packing in binuclear Fe(0)-M(II) (M=Hg, Cd) complexes with 2-(diphenylphosphino)thiazole. *J. Organomet. Chem.* **1999**, *575*, 51–56.

[30] Shields, Z. P.; Murray, J. S.; Politzer, P. Directional tendencies of halogen and hydrogen bonds. *Int. J. Quantum Chem.* **2010**, *110*, 2823–2832.

[31] Becke, A. D. Density-functional exchange-energy approximation with correct asymptotic behavior. *Phys. Rev. A*. **1988**, *38*, 3098.

[32] Valeur, B.; Leray, I. Design principles of fluorescent molecular sensors for cation recognition. *Coord.Chem. Rev.* **2000**, *205*, 3–40.

Supplemental Material: The online version of this article (DOI: 10.1515/hc-2015-0139) offers supplementary material, available to authorized users.